Hum Genet (2013) 132:91–105
DOI 10.1007/s00439-012-1228-5

ORIGINAL INVESTIGATION

Characterization of CCDC28B reveals its role in ciliogenesis and provides insight to understand its modifier effect on Bardet–Biedl syndrome

Magdalena Cardenas-Rodriguez · Daniel P. S. Osborn · Florencia Irigoín · Martín Graña · Héctor Romero · Philip L. Beales · Jose L. Badano

Received: 29 June 2012 / Accepted: 15 September 2012 / Published online: 27 September 2012

Abstract Bardet–Biedl syndrome (BBS) is a genetically heterogeneous disorder that is generally inherited in an autosomal recessive fashion. However, in some families, *trans* mutant alleles interact with the primary causal locus to modulate the penetrance and/or the expressivity of the phenotype. *CCDC28B* (*MGC1203*) was identified as a second site modifier of BBS encoding a protein of unknown function. Here we report the first functional characterization of this protein and show it affects ciliogenesis both in cultured cells and in vivo in zebrafish. Consistent with this biological role, our in silico analysis shows that the presence of *CCDC28B* homologous sequences is restricted to ciliated metazoa. Depletion of Ccdc28b in zebrafish results in defective ciliogenesis and consequently causes a number of phenotypes that are characteristic of BBS and other ciliopathy mutants including hydrocephalus, left–right axis determination defects and renal function impairment. Thus, this work reports CCDC28B as a novel protein involved in the process of ciliogenesis whilst providing functional insight into the cellular basis of its modifier effect in BBS patients.

Electronic supplementary material The online version of this article (doi:10.1007/s00439-012-1228-5) contains supplementary material, which is available to authorized users.

M. Cardenas-Rodriguez · F. Irigoín · J. L. Badano (✉)
Human Molecular Genetics Laboratory,
Institut Pasteur de Montevideo, Mataojo 2020,
11400 Montevideo, Uruguay
e-mail: jbadano@pasteur.edu.uy

D. P. S. Osborn · P. L. Beales
Molecular Medicine Unit, Institute of Child Health,
University College London, 30 Guilford St,
London WC1N 1EH, UK

F. Irigoín
Departamento de Histología y Embriología,
Facultad de Medicina, Universidad de la República, Montevideo,
Gral. Flores 2125, 11800 Montevideo, Uruguay

M. Graña
Bioinformatics Unit, Institut Pasteur de Montevideo,
Mataojo 2020, 11400 Montevideo, Uruguay

H. Romero
Laboratorio de Organización y Evolución del Genoma,
Facultad de Ciencias/C.U.R.E., Universidad de la República,
Iguá 4225, 11400 Montevideo, Uruguay

Introduction

Bardet–Biedl syndrome (BBS; OMIM 209900) is a rare genetic disorder characterized by retinal degeneration, obesity, learning difficulties, polydactyly and malformations of the gonads and kidneys (Beales et al. 1999). Several lines of evidence from both humans, animal and cellular models have indicated that BBS is caused by defects in the formation and/or function of primary cilia. Cilia are microtubule-based organelles organized from a basal body that emanate from the plasma membrane into the extracellular milieu acting as central hubs for signal processing, playing roles as mechano- and chemo-sensors and as transducers of different paracrine signaling cascades (Cardenas-Rodriguez and Badano 2009; Veland et al. 2009). Consequently, their disruption and/or dysfunction affects multiple cellular functions and thus have been causally associated not only with BBS but also with a number of human conditions collectively known as ciliopathies (Cardenas-Rodriguez and Badano 2009 and references within).

To date, seventeen BBS genes have been identified (*BBS1-12*, *MKS1*, *CEP290*, *FRITZ/C2ORF86*, *SDCCAG8*,

LZTFL1; Kim et al. 2010; Leitch et al. 2008; Marion et al. 2012; Otto et al. 2010 and references within). BBS is characterized by a significant inter- and intra-familiar phenotypic variability but although the former could be explained, at least in part, by the extensive genetic heterogeneity in the syndrome, these genotype-phenotype correlations have been difficult to establish. This is possibly due to the significant functional similarities among the BBS proteins as evidenced by cellular, biochemical and in vivo studies. The vast majority of BBS proteins characterized to date localize to centrosomes, basal bodies and the ciliary axoneme, and participate in ensuring the correct function of primary cilia (Ansley et al. 2003; Fan et al. 2004; Jin et al. 2010; Kim et al. 2004; Kim et al. 2005; Li et al. 2004; Loktev et al. 2008; Marion et al. 2009; May-Simera et al. 2009; Nachury et al. 2007). Seven BBS proteins (BBS1, 2, 4, 5, 7, 8, 9) have been shown to associate forming a complex termed the BBSome that participates in cilia biogenesis mediating the traffic of different cilia components towards the organelle (Jin et al. 2010; Loktev et al. 2008; Nachury et al. 2007; Veleri et al. 2012). Other BBS proteins form a separate complex of CCT/TRiC chaperonins and chaperonine like-BBS proteins (BBS6, 10, 12) that mediates the formation of the BBSome, thus affecting the same biological process albeit at a different level (Seo et al. 2010). In addition, the BBS proteins play a role in cilia-mediated paracrine signaling, affecting the transduction of the sonic hedgehog (Shh) and Wnt pathways (Gerdes et al. 2007; Ross et al. 2005; Wiens et al. 2010; Zhang et al. 2012).

As mentioned above, BBS is also characterized by extensive intra-familiar variability and it has been shown that in some families this phenomenon could be explained, at least in part, by oligogenic inheritance. Although some studies have not found clear indications of complex patterns of inheritance in BBS (Abu-Safieh et al. 2012; Laurier et al. 2006; Redin et al. 2012; Smaoui et al. 2006), other reports have shown that mutations at more than one BBS locus segregate with the disease modulating either its penetrance or expressivity (Badano et al. 2003; Beales et al. 2003; Bin et al. 2009; Katsanis et al. 2001; Leitch et al. 2008; Stoetzel et al. 2006). Thus, at least in some families, this characteristic phenotypic variability could be due to a different mutational load in cilia-associated genes among siblings. *CCDC28B* (coiled coil domain containing protein 28B; also named *MGC1203*) was identified originally as a second site modifier of BBS, whereby reduced levels of *CCDC28B* mRNA in a sensitized genetic background, i.e., in the presence of mutations at other BBS loci, correlate with a more severe presentation of the disease (Badano et al. 2006). However, the contribution of *CCDC28B* mutations to modulate the BBS phenotype is still not clear (for example see Abu-Safieh et al. 2012; Bin et al. 2009; Redin et al. 2012).

CCDC28B encodes a coiled coil containing protein that has been shown to interact with several BBS proteins (Badano et al. 2006). Little is known about the possible functions of CCDC28B, and thus, the cellular basis of its putative modifier effect. Here we show that CCDC28B homologous sequences are restricted to metazoa, all of which are ciliated organisms. We show that the protein plays a role in ciliogenesis whereby both knockdown of CCDC28B in cells and in vivo in zebrafish results in fewer and/or shorter cilia. Consequently, zebrafish *ccdc28b* morphant animals present a number of phenotypes that are characteristic of other BBS and ciliopathy mutants. Thus, this work documents the first functional link between this BBS associated gene and ciliogenesis and provides insight to understand the cellular basis of its modifier effect.

Materials and methods

Sequence searches and phylogenetic analyses

First, the existence of CCDC28B homologous sequences with known three-dimensional structures was ruled out using HHpred (Söding 2005). Next, the NR sequence databases from NCBI were scanned with a set of profile-based methods, namely CS-Blast (Biegert and Söding 2009), HHblits (Remmert et al. 2011) and HHsenser (Söding et al. 2006). All methods were run both individually as well as in combined forms, i.e., using significant results from one given method as the input for another one. The complete and curated metazoan proteomes stored at UniProt (as to June 2012, $n = 85$, see supplementary material for complete list; The Uniprot Consortium 2012) were queried with the human CCDC28B protein sequence using Blastp (Altschul et al. 1990). The *Petromyzon marinus* (lamprey) proteome and the exon–intron structure shown in Fig. 1 were retrieved from Ensembl (Flicek et al. 2011). Positive hits were then aligned with T-Coffee (Notredame et al. 2000), Prank (Loytynoja and Goldman 2005) and Mafft (Katoh et al. 2002). Maximum-likelihood phylogenetic trees were computed with PhyML (Guindon and Gascuel 2003) with default parameters.

Morpholino and rescue experiments

The splice morpholino (MOSpl) against *ccdc28b* and the standard control morpholino were obtained from Gene Tools. To determine the working dose we performed RT-

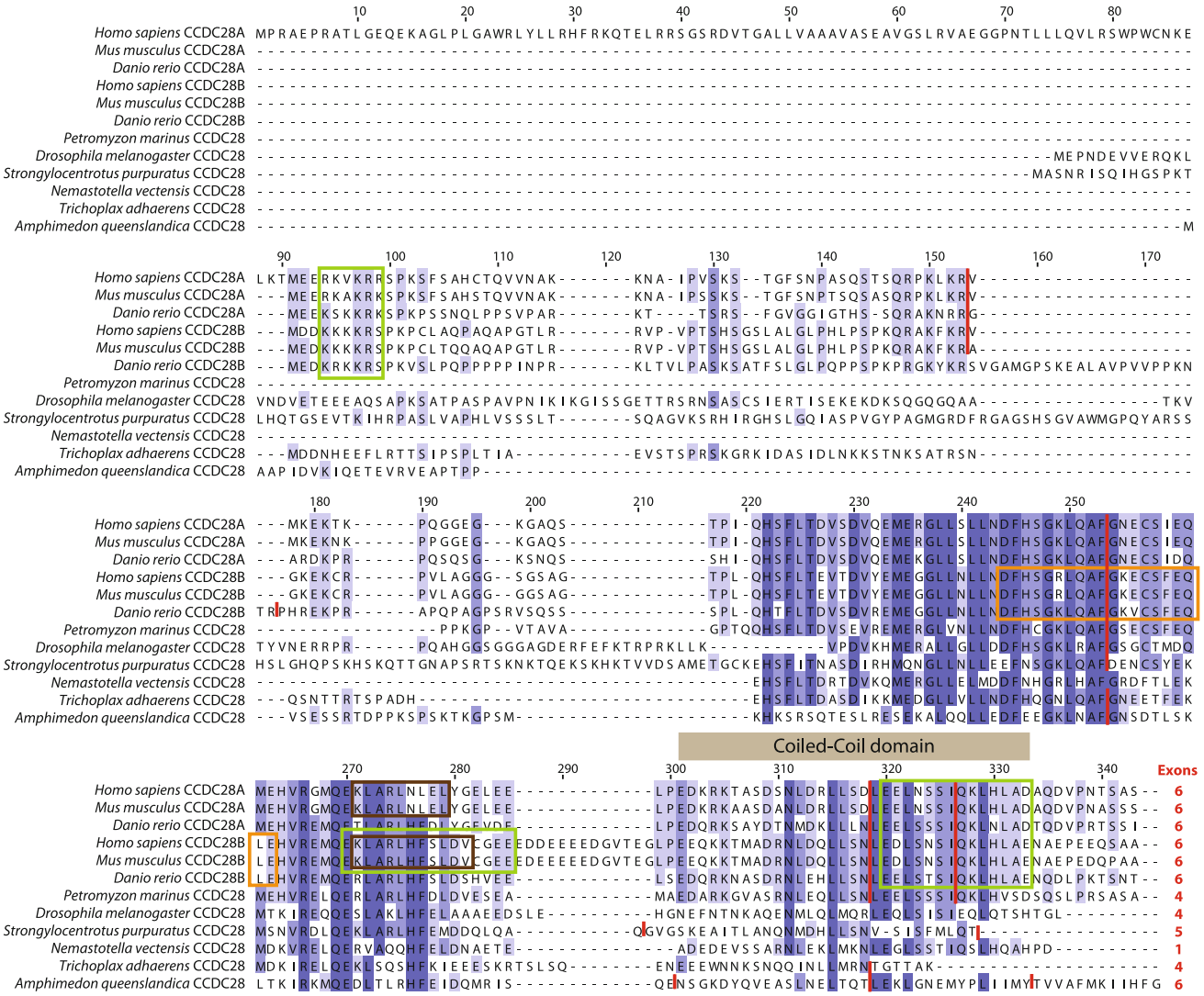

Fig. 1 CCDC28B is a conserved coiled coil protein. Schematic representation of the amino acid sequence of human CCDC28B aligned to orthologous sequences of *Mus musculus*, and *Danio rerio*, CCDC28A from human, mouse and zebrafish, and CCDC28 from *Petromyzon marinus*, *Drosophila melanogaster*, *Strongylocentrotus purpuratus*, *Nemastotella vectensis*, *Trichoplax adhaerens* and *Amphimedon queenslandica*, denoting the percentage identity at each position. The alignment was performed using Jalview (Waterhouse et al. 2009). The approximate boundaries of different protein domains and putative motifs are highlighted. CCDC28B is predicted to have both a NLS (N-terminal; *green box*) and two NES motifs (middle and C-terminal; *green box*). The location and conservation of a putative calmodulin IQ binding motif (*orange box*) and a MAPK docking motif (*brown box*) is also shown. *Red vertical lines* indicate the position of the exon boundaries and the total number of exons for each species is also shown

PCR (primers are available upon request) using total RNA extracted from morphant embryos. RNA was extracted from 25–30 embryos using the TRIzol reagent (Invitrogen) and cDNA was prepared using the SuperScript First-Strand Synthesis System for RT-PCR (Invitrogen). We injected wild type zebrafish embryos at a one- to two-cell stage with 0.5–1 nanoliters of morpholino solutions prepared to deliver the concentrations stated in the text. Morpholino sequence: *ccdc28b* MOSpl: TTTAGAAGACGCACACAAACCTTGT (exon 2-intron 2 junction). For rescue experiments, we cloned the full-length zebrafish *ccdc28b* ORF into pCS2 and prepared mRNA using the Ambion mMessage mMachine SP6 kit.

Zebrafish assays

Cartilage staining

We treated embryos from 8 hpf with PTU (1-phenyl 2-thiourea) for depigmentation and then stained with Alcian Blue at 5 dpf as described (Tobin et al. 2008). We measured the ceratohyal cartilage angles using ImageJ.

Phalloidin staining

We fixed 48–72 h embryos in 4 % paraformaldehyde (PFA), washed with 1 % Tween in PBS and cold acetone. We incubated embryos with phalloidin-rhodamine (Invitrogen) for 30 min at room temperature, washed with 1 % Tween-PBS, and mounted with Citifluor mounting media (Citifluor Ltd.) for confocal imaging.

Renal function assay

We injected rhodamine dextran (Invitrogen) into the pericardium of PTU treated control and morphant animals at 72 hpf. Given the size of the pronephric ducts, the requirement of confocal microscopy, and the need to maintain embryos alive during the course of the experiment, we choose to image the heart region using an epifluorescent microscope to monitor the decay in fluorescence in the general circulation as an indicator of renal function. We took images of the heart region of at least 10 embryos per condition tested, both 3 and 24 h post-injection. The same embryo is compared at 3 and 24 hpi thus controlling for possible differences in the starting amount of dye. Total fluorescence was measured using ImageJ. We noted normal heart rate and full circulatory movement to ensure that the lack of fluorescence was not due to poor blood circulation.

Cilia analysis

We used γ- and acetylated α-Tubulin antibodies (Sigma) and isotype specific secondary antibodies (Invitrogen). We used a Zeiss LSM 710 confocal microscope.

RNA in situ hybridization

Performed using standard protocols. Antisense and sense *ccdc28b* probes were synthesized from full-length T7-incorporated PCR products (primer sequences available on request).

Cell culture and Stealth RNAi

We maintained hTERT-RPE cells in a 1:1 mix of Dulbecco's modified Eagle medium (DMEM) and F12 (Invitrogen) supplemented with 10 % fetal bovine serum and 0.01 mg/ml hygromicin B, at 37 °C in 5 % CO_2. We transfected cells using RNAiMax following the manufacturers recommendations (Invitrogen). Stealth RNAi oligos were obtained from Invitrogen. Control cells were transfected with a Stealth RNAi Low GC Negative Control duplex as it matched the GC percentage of the *CCDC28B* and *IFT88* targeting duplexes. The efficiency of knockdown for each gene was evaluated by real time PCR using SYBR green (Quantimix Easy SYG KIT; BioTools) and using *GAPDH* for normalization. Fold change in expression of *IFT88* and *CCDC28B* between knockdown cells and controls was calculated as $2^{-\Delta\Delta Ct}$ as described (Gascue et al. 2012). Oligos and Stealth RNAi sequences are available upon request.

Results

CCDC28B is a coiled coil containing protein conserved in ciliated metazoa

To begin the characterization of CCDC28B we first evaluated its presence and level of conservation across species. *CCDC28B* encodes a protein of 200 amino acids (NP_077272). To detect homologous sequences to NP_077272, we carried out intensive database searches (see Methods). Combining significant matches from all these searches resulted in a set of sequences with no representatives from Prokaryote (Bacteria/Achaea), Plant or Fungi. Next, eukaryotic protein sequences were used to build a phylogenetic tree. Dismissing minor disagreements with established taxonomic classifications, tree topologies were consistent for the different alignment algorithms. Overall, and albeit the existence of CCDC28B-like proteins in other phyla cannot be discarded, our analysis shows that unambiguous CCDC28B homologs are confined to metazoa, including porifera, cnidaria and placozoa (Supp. Fig. 1). Restricting our analysis to species with completely sequenced and annotated genomes, we were unable to find CCDC28B homologs in nematodes (nine species, including *C. elegans*), and platyhelminthes (two species). Interestingly, the absence of CCDC28B homologs in nematodes appears to be the result of a specific loss given that CCDC28B is present in Arthropoda (also members of the Ecdysozoa clade).

A salient feature of the dendrogram is the apparent ancestral gene duplication of CCDC28 in vertebrates. Our phylogenetic analysis indicates that a duplication that took place sometime between the divergence of lamprey, which shows a single CCDC28 protein, and the appearance of Teleostomi, gave rise to two paralogs: CCDC28A and CCDC28B (Fig. 1; Supp. Fig. 1). *CCDC28A* encodes a protein of 274 amino acids (NP_056254) that has been shown to encode two isoforms: a long isoform in which the first 90 residues of the protein are poorly conserved, and a short isoform, composed of the remaining 184 amino acids, that is highly conserved in vertebrates (Petit et al. 2012; Fig. 1). The amino acid alignment demonstrates a high level of conservation between CCDC28B and the short isoform of CCDC28A across species (Fig. 1; for a complete alignment of all available sequences see Supp.

Fig. 2). Our phylogenetic analysis shows that both genes are evolving at comparable speeds although subtle differences cannot be excluded (Supp. Fig. 1). Furthermore, the exon–intron structure of both genes is also conserved, with six exons in Teleostomi while the lamprey and Drosophila present four exons (Fig. 1).

Next we analyzed the amino acid sequence of CCDC28B in an effort to delineate putative protein motifs that could provide functional information. As expected, CCDC28B presents a coiled coil domain located in the C-terminal region of the protein, between residues Glu158 and Glu193 (http://www.ch.embnet.org/software/COILS_form.html; Lupas et al. 1991). These domains typically mediate protein oligomerization and/or heterologous protein–protein interactions (Burkhard et al. 2001). In contrast, the N-terminal region of the protein, comprising the first 75–80 amino acids, is predicted to be disordered (http://bioinf.cs.ucl.ac.uk/disopred; Ward et al. 2004).

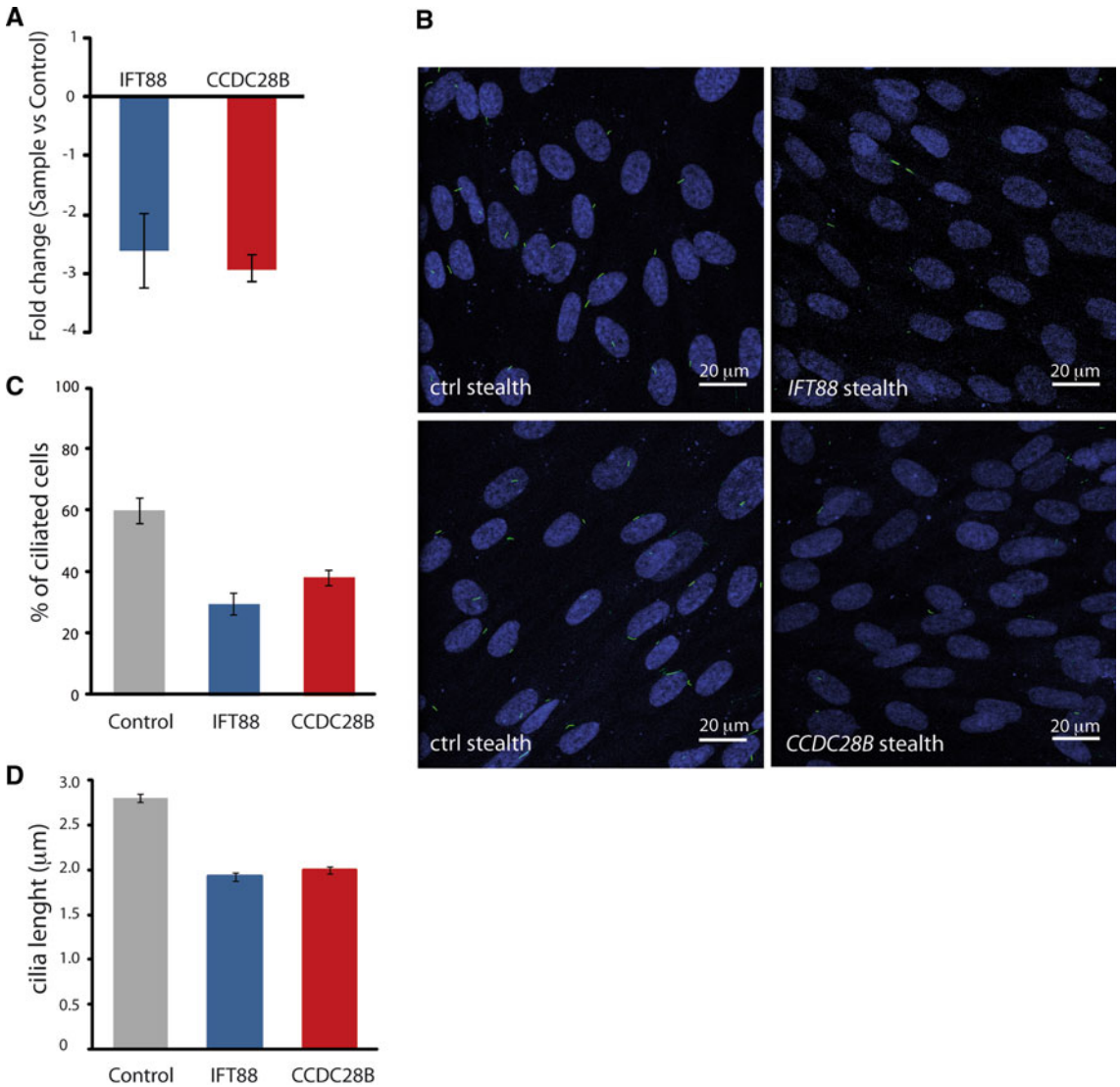

Fig. 2 Depletion of CCDC28B in hTERT-RPE cells results in ciliogenesis defects. **a** Real time PCR showing the efficiency of knockdown of the *IFT88* and *CCDC28B* stealth RNA oligos. *GAPDH* was used for normalization. The relative expression of each gene is shown as fold change ($2^{-\Delta\Delta Ct}$) between samples (stealth RNAi oligos) and controls (Low GC Stealth RNAi control). *Error bars* correspond to standard deviation from biological and technical duplicates. **b** Confocal images of hTERT-RPE cells transfected either with the Low GC Stealth RNAi control or with the RNAi oligos targeting *CCDC28B* and *IFT88,* showing a decrease in the number of ciliated cells. TOPRO (*blue*) and acetylated tubulin (*green*) were used to visualized nuclei and cilia, respectively. **c** In excess of 100 cells were counted and scored for the presence of cilia. The percentage of ciliated cells in each condition was quantified. *Error bars* correspond to SEM; $P < 0.001$. **d** Cilia length was measured in more than 300 cilia from controls and cells depleted for IFT88 and CCDC28B. *Error bars* correspond to SEM; $P < 0.001$

Interestingly, centrosomes and cilia have been shown to be heavily enriched in proteins with both coiled coil motifs and intrinsically disordered regions (Nido et al. 2012). Analyzing the protein with The Eukaryotic Linear Motif resource for Functional Sites in Proteins (ELM; http://elm.eu.org/; Dinkel et al. 2012) showed similar results regarding the coiled coil and disordered region and also predicted several potentially relevant functional domains. For example CCDC28B is predicted to present a calmodulin binding IQ motif located between the residues D101 and E120, a mitogen-activated protein kinase (MAPK) docking motif between K128 and V138, and both a nuclear localization signal (NLS) at the N-ter and two nuclear export signals (NES) centered on F134 and D178. CCDC28A is also predicted to have the N-terminal NLS, the C-terminal NES and the MAPK motifs while is not predicted to have the IQ motif and central NES due to single amino acid changes.

CCDC28B affects ciliogenesis in cultured hTERT-RPE cells

We then started the functional analysis of CCDC28B by testing whether it plays a role in ciliogenesis in a cell-based assay using the ciliated human cell line hTERT-RPE (retinal pigmented epithelial cells). We performed the CCDC28B knockdown in these cells using the Stealth RNAi system. We transfected a double stranded Stealth RNA oligo targeting *CCDC28B* alongside with the corresponding control RNA (Low GC control). We also used a Stealth RNA oligo targeting a gene known to be required for ciliogenesis, as it is the intraflagellar transport gene *IFT88*, to provide a reference value for our cell-based assay in which we attempted to maximize the percentage of ciliated cells by adjusting the ratio between transfection efficiency and cell culture confluency. We first determined whether our Stealth RNA oligos effectively reduced *CCDC28B* and *IFT88* levels by real time PCR (Fig. 2a). We then transfected hTERT-RPE cells with our RNA oligos and measured the percentage of ciliated cells and the average ciliary length in controls, *CCDC28B* and *IFT88* knockdown cells. We observed a significant reduction in both the number and length of cilia upon knockdown of *CCDC28B*. While 60 ± 4 % of control cells were ciliated with an average length of 2.80 ± 0.05 µm, only 38.3 ± 3.4 % cells transfected with the *CCDC28B* stealth oligo presented cilia with an average length of 1.99 ± 0.04 µm, a reduction that was comparable to the effect obtained in *IFT88* depleted cells (29.7 ± 2.4 % of ciliated cells with an average length of 1.93 ± 0.04 µm; $P < 0.001$; Fig. 2b–d). Thus our results show that *CCDC28B* affects ciliogenesis in this system.

Zebrafish *ccdc28b* morphant embryos present cilia-related phenotypes

In zebrafish, there is a single ortholog of *CCDC28B* (NM_001145573.1, NP_001139045; reciprocal best hit; 55 % identity and 65 % similarity; Fig. 1) that is expressed both maternally and zygotically in a ubiquitous manner along the rostrocaudal axis (Badano et al. 2006; Fig. 3a). To knock down the protein levels of Ccdc28b we designed a splice blocking morpholino (MOspl) targeting the exon 2-intron 2 junction in *ccdc28b*. The retention of intron 2 (90 bp) changes the open reading frame and introduces a premature stop codon 17 bp into the intron. Thus, the aberrantly spliced *ccdc28b* mRNA, if translated, could encode a truncated protein representing only the first 79 residues of a 213 amino acid protein. To check the efficiency of our knockdown we performed RT-PCR using RNA from control and morphant embryos. Amplification from the wild type, fully spliced mRNA, results in a 233 bp band whereas the targeted *ccdc28b* mRNA, retaining intron 2, generates a 323 bp PCR product. We could observe that the MOspl efficiently affected the splicing of *ccdc28b* in a dose-dependent fashion (Fig. 3b) and both the number (data not shown) and severity of affected embryos correlated with the concentration of MOspl injected (Fig. 3c). Importantly, injecting 3 ng of *ccdc28b* MOspl was not sufficient to fully disrupt the correct splicing of the mRNA (Fig. 3b); injecting higher doses of morpholino resulted in gastrulation arrest and lethality in nearly 100 % of injected embryos, suggesting that a minimum level of Ccdc28b is required to complete early developmental stages and maintain viability. Using 3 ng of *ccdc28b* MOspl, which therefore reduces but does not abolish the amount of Ccdc28b, consistently yielded in excess of 80 % of affected embryos and thus we selected this dose for subsequent studies. The morphant phenotype is specific since it can be fully rescued by injecting mature *ccdc28b* mRNA which by itself does not produce an appreciable phenotype (Fig. 3e).

We therefore injected 3 ng of *ccdc28b* MOSpl and assessed the phenotype of morphants embryos starting at 10 h post fertilization (hpf) and up to 72 hpf. *Ccdc28b* morphants were characterized by a shortening of the body axis, poor somitic definition, an increase in body curvature, smaller eyes, defects in the pattern of pigmentation and craniofacial alterations (Fig. 3c–e). *Ccdc28b* morphants also present with hydrocephalus, visible as a swelling of the fourth ventricle in live embryos or as a depression in fixed animals due to dehydration (Fig. 4a; arrows). Thus, depletion of Ccdc28b in zebrafish resulted in a number of phenotypes that are observed in other BBS and ciliary mutants and morphants (Badano et al. 2006; Gerdes et al. 2007; Ross et al. 2005; Tobin et al. 2008; Walczak-Sztulpa et al. 2010; Yen et al. 2006).

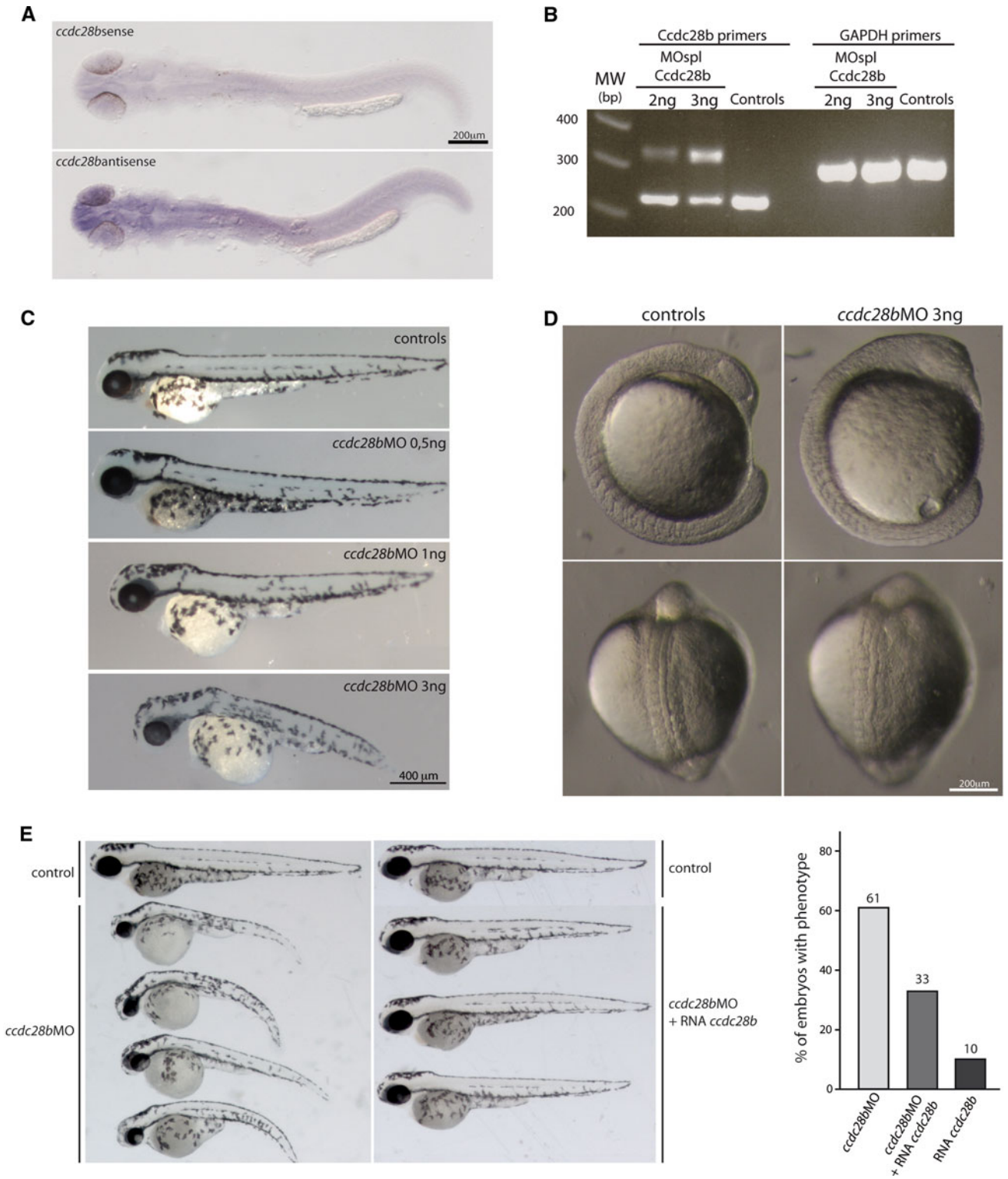

Fig. 3 Phenotypic characterization of *ccdc28b* morphant embryos. **a** RNA in situ hybridization showing ubiquitous expression of *ccdc28b* along the rostrocaudal axis. **b** RT-PCR analysis of *ccdc28b* mRNA levels showing a dose-dependent increase in the levels of unspliced messenger. *Gapdh* was used as control. **c** Gross morphology of *ccdc28b* morphants using increasing doses of MO. Affected embryos present with defects in the pigmentation pattern, smaller eyes, a shorter/curved body axis and craniofacial malformations. **d** Side and top views of control and *ccdc28b* morphant embryos at 10 somite-stage showing poorly defined somites in our morphants. **e** The *ccdc28b* morphant phenotype is fully rescued by the injection of zebrafish *ccdc28b* mRNA

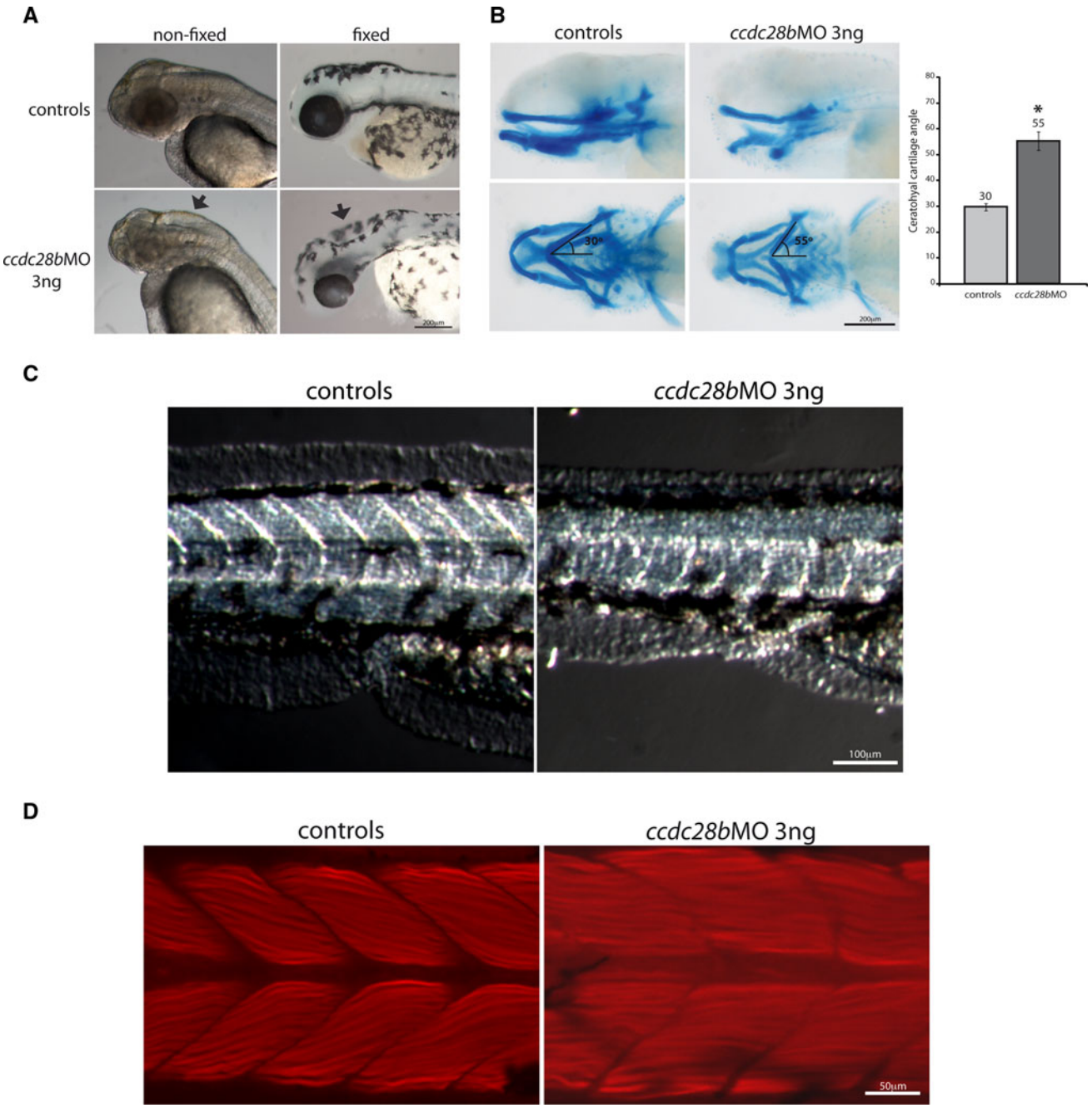

Fig. 4 *Ccdc28b* morphants present hydrocephalus, craniofacial defects and actin disorganization. **a** Hydrocephalus was evident in live *ccdc28b* morphants as a swelling of the fourth ventricle (*arrows*). After fixation, and due to dehydration, the phenotype is observed as a depression (*arrow*). **b** Alcian blue staining of cartilage showing that *ccdc28b* morphants present with craniofacial defects. *Error bars* correspond to SEM; $P < 0.001$. **c** Bright field images of the tail region showing a disorganization of somitic structure in *ccdc28b* morphant embryos. **d** F-actin in the somite region of both control and *ccdc28b* morphants was observed with phalloidin staining. Morphant animals present disorganization of the actin fibers

BBS patients, mouse BBS models, and zebrafish *bbs* morphants present with craniofacial defects due to impaired neural crest cell migration (Tobin et al. 2008). To characterize this defect further in our *ccdc28b* morphants we stained cartilage with alcian blue and measured the angle of the ceratohyal cartilage. We observed a significant increase in the angle from $30° \pm 1.4$ in controls to $55° \pm 3.6°$ in morphants ($P < 0.001$; Fig. 4b). *Ccdc28b* morphants also present with poor somitic definition (Figs. 3d, 4c), which we characterized further by visualizing muscle F-actin fibers by phalloidin staining and confocal imaging. Observing the actin distribution at

comparables planes between control and morphants we observed a marked phenotype upon knockdown of Ccdc28b. In contrast to controls, where the array of actin filaments is well organized, muscle fibers in *ccdc28b* morphants presented disrupted actin bundles (Fig. 4d) similar to what has been reported for *bbs8* morphants (May-Simera et al. 2010).

Ciliogenesis is perturbed in *ccdc28b* morphants

Given that CCDC28B affects ciliogenesis in cells and the overall phenotype of *ccdc28b* morphants is compatible with a defect in ciliary function we next tested whether these organelles are affected in these embryos. To test this possibility we first assessed cilia in the Kupffer's vesicle (KV), a transient ciliated structure responsible for establishing the left–right axis of symmetry (Essner et al. 2005). To visualize KV cilia we used confocal microscopy using antibodies against γ- and acetylated tubulin (staining basal bodies and cilia, respectively). We analyzed in excess of 500 cilia from 18 individual KVs of both age-matched (8 somite stage) controls and morphants. We observed that injection of *ccdc28b* MOSpl resulted in a significant reduction in the length of KV cilia (3.24 ± 0.13 μm) compared to controls (4.65 ± 0.21 μm) showing that ciliogenesis is impaired in our morphants (Fig. 5a). However, the number of cilia was not significantly altered in the KV of our morphant embryos (data not shown) likely highlighting important differences between ciliogenesis in RPE cells and in vivo. As mentioned earlier, cilia motility and the generation of extracellular fluid flow in the KV have been shown to be required to break the left–right axis of symmetry. Therefore, we next tested whether this KV ciliary phenotype translates into a defect in axis specification in *ccdc28b* morphants. We performed RNA in situ hybridization using an antisense probe to cardiac myosin light chain 2 (*cmlc2*) to visualize heart looping in both control and morphant embryos. While 35 out of 36 control embryos (97 %) were normal, 14 out of 34 morphant embryos (41 %) presented defective looping (middle position or right looping; Fig. 5b) showing that the defect in KV ciliogenesis disrupts left–right axis specification in our morphant embryos.

To further evaluate this ciliogenesis defect in *ccdc28b* morphants we examined other ciliated tissues. We first stained for cilia and observed the epithelium lining the pronephric ducts. In control embryos, cilia are aligned along the duct and are thus visualized as a thin line (Fig. 6a, upper panel). In contrast, although cilia length in this tissue was difficult to document, the cilia organization in *ccdc28b* morphant was clearly perturbed (Fig. 6a, lower panel). Cilia in the zebrafish pronephros are motile and both their immotility or uncoordinated movement have been shown to result in renal defects and cyst formation often associated with ciliogenesis and developmental defects at the cloaca leading to obstruction (Kramer-Zucker et al. 2005). To assess whether the cilia defect in our *ccdc28b* morphants affects renal function we performed a rhodamine dextran clearance assay injecting dye into the pericardium and monitoring the decay in fluorescence with time. At 24 h post-injection control animals retained 38 ± 6 % of the dye while *ccdc28b* morphants retained 82 ± 3 % of the dye, indicating defective renal function ($P < 0.001$; Fig. 6b). However, we did not detect the formation of cysts in *ccdc28b* morphants possibly due to the absence of an obstruction at the cloaca and likely residual activity of Ccdc28b. Importantly, dye uptake was similar between morphants and controls, as evidenced by images at 3 hpi (Fig. 6b), indicating that the observed differences are not due to defects in circulation. Next, we looked at the olfactory pit, another heavily ciliated tissue. While the size of the olfactory pit was comparable to that of controls, basal bodies and cilia in *ccdc28b* morphants appeared disorganized (Fig. 6c). Thus our results show that depletion of Ccdc28b results in defective KV ciliogenesis and disorganization of cilia both in the pronephros and olfactory pit.

Discussion

Here, we report the characterization of the BBS second site modifier CCDC28B. Knockdown of Ccdc28b in zebrafish resulted in a set of phenotypes that are reminiscent of different ciliary morphants and BBS mutants (Badano et al. 2006; Gerdes et al. 2007; Ross et al. 2005; Tobin et al. 2008; Walczak-Sztulpa et al. 2010; Yen et al. 2006). For example defective retrograde melanosome transport in *bbs* morphants resulted in pigmentation defects similar to those observed in *ccdc28b* morphants (Yen et al. 2006). Likewise, the skeletal defects of *ccdc28b* morphants resemble the craniofacial malformations (observed in BBS animal models and patients) that are caused by aberrant neural crest cell migration (Tobin et al. 2008). Another cilia-associated phenotype is hydrocephalus, a condition caused typically by defective motility of cilia in the epithelium lining the brain ventricles (Ibanez-Tallon et al. 2004). Furthermore, we show that *ccdc28b* morphant embryos present defective ciliogenesis and/or cilia organization defects in different ciliated tissues, a phenotype that likely explains the aforementioned conditions. Notably, knockdown of individual BBS genes in both mice and cells does not necessarily result in ciliogenesis defects. *Bbs2*, *Bbs4* and *Bbs6* knockout mice are able to form cilia (Fath et al. 2005; Mykytyn et al. 2004; Nishimura et al. 2004), while knockdown of several BBSome components do not affect

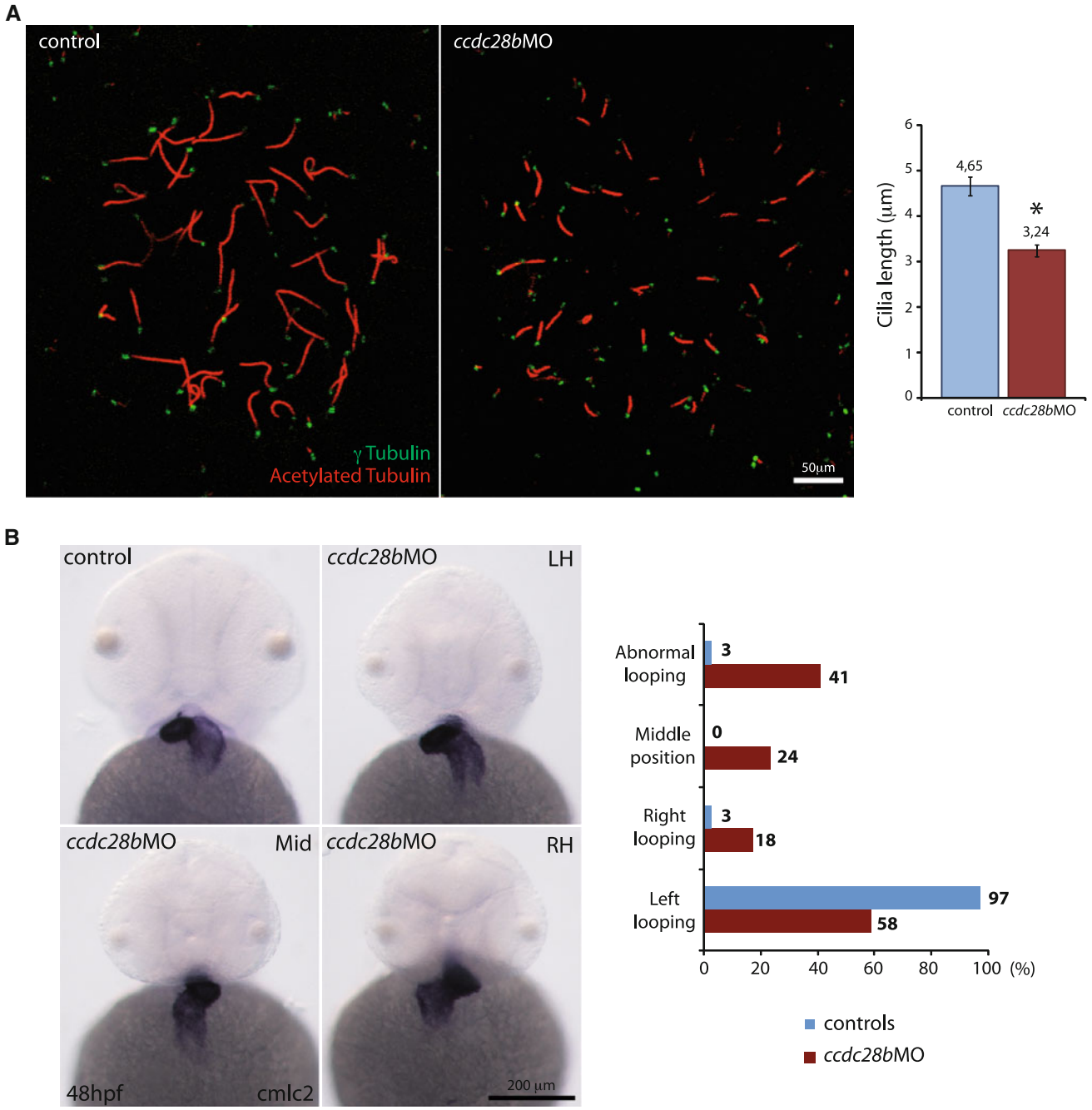

Fig. 5 Knockdown of Ccdc28b results in KV ciliogenesis and L–R axis determination defects. **a** Cilia and basal bodies in the KV were visualized by staining with acetylated (*red*) and γ-tubulin (*green*), respectively. Confocal images were processed and the length of cilia was measured using ImageJ. The average cilia length in *ccdc28b* morphants is significantly shorter than in control animals. *Error bars* correspond to SEM; $P < 0.001$. **b** RNA in situ hybridization using a probe for the cardiac marker cmlc2 shows that morphant animals present defective L–R axis specification

ciliogenesis in hTERT-RPE cells (Loktev et al. 2008). These data could indicate that the function of CCDC28B might be at least partially different from that of *bona fide* BBS proteins. Given that CCDC28B physically interacts with a number of BBS proteins, including different members of the BBSome, one possibility is that CCDC28B might facilitate or mediate BBSome function, thus affecting the function of the complex as a whole. In this scenario, and considering the possibility of at least partial functional redundancy among the BBS protein, it would be expected that depletion of CCDC28B might have a more profound impact on ciliogenesis than the removal of individual BBS moieties. In addition, CCDC28B might have BBSome independent functions related to cilia biology.

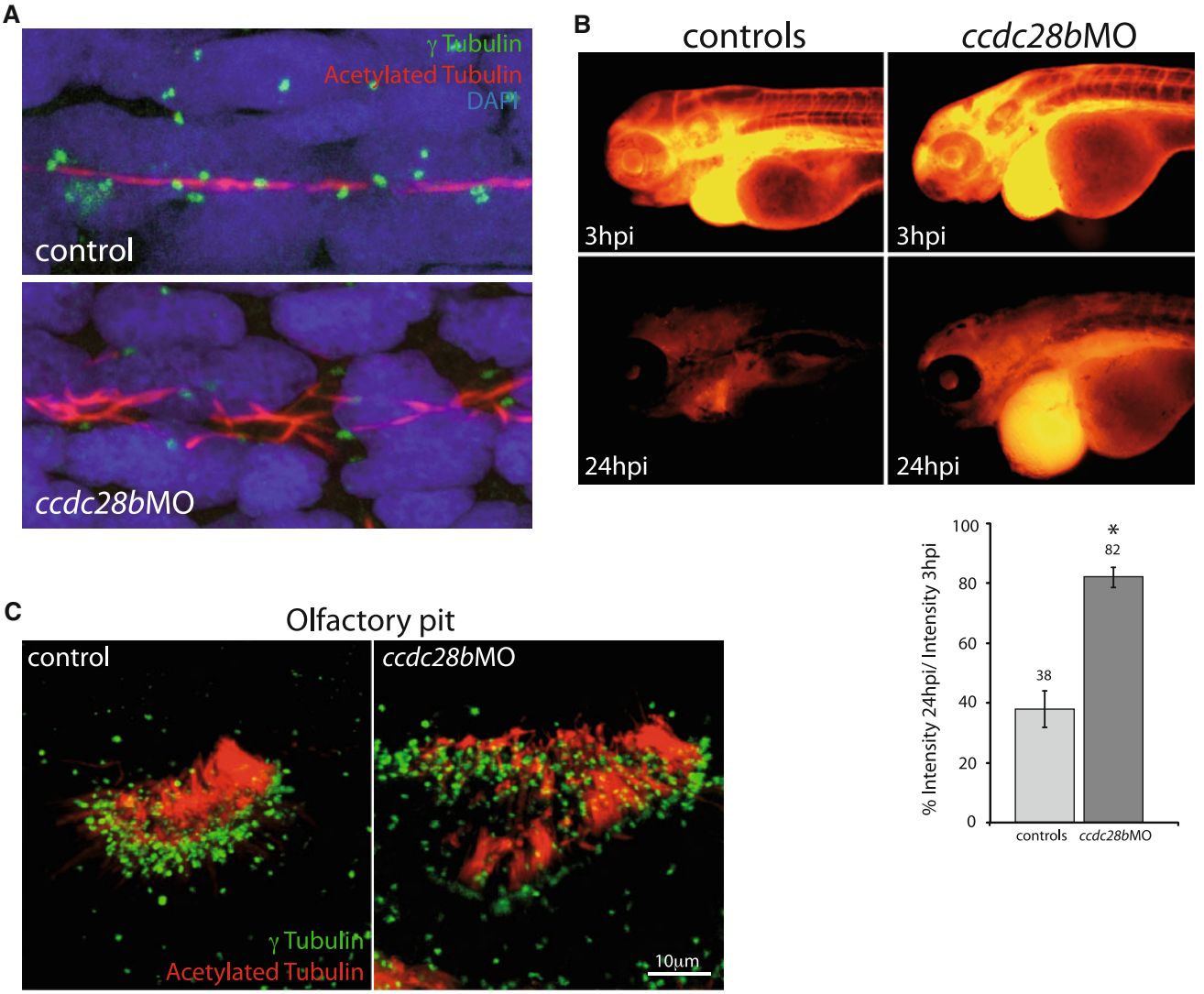

Fig. 6 *ccdc28b* morphants present cilia organization defects. **a** Basal bodies (γ-Tubulin; *green*), cilia (acetylated Tubulin; *red*) and nuclei (DAPI; *blue*) were observed in the pronephric ducts of control and *ccdc28b* morphants. Morphant animals presented disorganized cilia. **b** A rhodamine dextran clearance assay shows that *ccdc28b* morphants presented reduced rates of excretion of the dye. *Error bars* correspond to SEM; $P < 0.001$. **c** While the size and morphology of the olfactory pit is not severely affected in *ccdc28b* morphant embryos, the organization of cilia is altered

The analysis of the CCDC28B sequence identified some putative motifs that might be relevant to its function both in cilia biology and potentially outside of the organelle. For example, CCDC28B is predicted to have both NLS and NES motifs suggesting that it could shuttle in and out of the nucleus. We have shown recently that some BBS protein play a nuclear role whereby they affect gene transcription through an interaction with RNF2, a chromatin remodeling protein (Gascue et al. 2012). Further studies will be required to test whether CCDC28B has the capacity to enter the nucleus and whether these putative motifs participate in the process. Regarding its role in ciliogenesis, CCDC28B is predicted to possess both a calmodulin binding IQ motif and a MAPK docking motif. Calmodulin mediates Ca^{2+} signaling thus regulating diverse cellular processes such as, for example, cytoskeletal reorganization (Bähler and Rhoads 2002) that could in turn affect both ciliogenesis directly as well as the organization of ciliated tissues, phenotypes that are observed upon knockdown of Ccdc28b. Furthermore, IQ motifs are targets for the activity of protein kinases such as PKA and PKC, which not only have a role in regulating the cytoskeleton but also have been shown recently to participate in ciliogenesis together with the MAPK cascade (Abdul-Majeed et al. 2012; Bähler and Rhoads 2002). Further studies will be required to validate and analyze the biological relevance of these CCDC28B putative motifs and to dissect whether CCDC28B plays a broader role in cytoskeletal organization.

Our phylogenetic analysis is also consistent with a role of this protein in ciliary biology since all the CCDC28B homologous sequences that we were able to find belong to ciliated organisms. In contrast, we could not detect clear-cut homologies in Prokaryotes, Fungi or Plants. Although failed detection does not prove inexistence of the protein in such vast taxonomic groups, our results are robust using state-of-the-art methods and permit speculation on the likely evolutionary origins of CCDC28B. CCDC28B appears to be confined to multicellular metazoa that are ciliated but is not present in every ciliated organism. It is therefore tempting to speculate that CCDC28B might represent a protein that, although not strictly required to form cilia or flagella, might play an important ciliary function in the context of multicellular organisms. Interestingly, remote homologs (not included in the presented phylogram) are from ancient eukaryotes that preceded multicellular metazoans. Such taxa, namely *Dictyostelium* sp. and *Capsaspora owczarzaki*, display today cellular/molecular intricacies that may have paved the way for evolutionary complexity. Our analysis also shows that *CCDC28* suffered a duplication event in vertebrates to give rise to *CCDC28A* and *CCDC28B*. CCDC28A has been linked to hematopoietic development and to the pathogenesis of different types of leukemia as a fusion protein with the nucleoporin NUP98 (Petit et al. 2012). Given the high conservation between the two CCDC28 proteins, it would be interesting to test whether CCDC28A also plays a role in cilia biology. However, the fact that knockdown of CCDC28B, in both cells and zebrafish, results in clear ciliary phenotypes indicates that the two proteins are not likely to be functionally redundant, at least in the context of ciliogenesis. Interestingly, the duplication event that originated *CCDC28A* and *CCDC28B* coincides with the proposed increase in the functional complexity associated with cilia in vertebrates (Davis et al. 2006). Thus, and similarly to what has been proposed for the vertebrate specific chaperonins BBS6, BBS10 and BBS12 (Stoetzel et al. 2007), it could be possible that proteins such as CCDC28B might have evolved to play a role facilitating the acquisition of novel functions by the cilium. More thorough analyses should be carried out to build on our results and unravel the intricacies of the evolutionary history of these genes and proteins.

Our data therefore show that CCDC28B regulates ciliogenesis and we have shown previously that this gene acts as a second site modifier in some BBS families (Badano et al. 2006). However, there are no reports of mutations in *CCDC28B* being sufficient to cause BBS or other ciliopathies in humans. One explanation is that complete loss of function of *CCDC28B* might be either associated with more severe ciliopathies or incompatible with life. Supporting these possibilities it is important to note that the alteration that we have reported previously in BBS patients is likely a hypomorphic mutation that results from a synonymous change affecting the normal splicing of the *CCDC28B* mRNA that leads to reduced levels of wild type mRNA (Badano et al. 2006). In addition, our data shows that injecting MOspl doses above 3 ng in zebrafish resulted in developmental arrest and death with a 100 % penetrance. Thus, an interesting possibility is that *CCDC28B* might contribute causal alleles to other, more severe, ciliopathies such as Meckel-Gruber syndrome (MKS), a scenario that would be reminiscent of the genetic overlap between MKS and BBS whereby hypomorphic mutations in MKS genes have been found in BBS patients (Leitch et al. 2008). Further work will be needed to continue dissecting the biological role of CCDC28B and to understand the mechanism by which it affects cilia biogenesis.

Acknowledgments We thank Paola Lepanto for her assistance in image analysis and the Badano and Beales laboratory members for discussions and technical help. This study was supported by ANII-Innova and the Genzyme Renal Innovations Program (GRIP) (JLB) and by a grant EU FP7 (SYSCILIA-241955) to PLB and DO. JLB, MC-R, MG, HR and FI are supported by the "Programa de Desarrollo de las Ciencias Básicas", PEDECIBA, and by the Agencia Nacional de Investigación e Innovación (ANII), Uruguay. PLB is a Wellcome Trust Senior Research Fellow.

References

Abdul-Majeed S, Moloney BC, Nauli SM (2012) Mechanisms regulating cilia growth and cilia function in endothelial cells. Cell Mol Life Sci 69:165–173

Abu-Safieh L, Al-Anazi S, Al-Abdi L, Hashem M, Alkuraya H, Alamr M, Sirelkhatim MO, Al-Hassnan Z, Alkuraya B, Mohamed JY, Al-Salem A, Alrashed M, Faqeih E, Softah A, Al-Hashem A, Wali S, Rahbeeni Z, Alsayed M, Khan AO, Al-Gazali L, Taschner PE, Al-Hazzaa S, Alkuraya FS (2012) In search of triallelism in Bardet-Biedl syndrome. Eur J Hum Genet 20:420–427

Altschul SF, Gish W, Miller W, Myers EW, Lipman DJ (1990) Basic local alignment search tool. J Mol Biol 215:403–410

Ansley SJ, Badano JL, Blacque OE, Hill J, Hoskins BE, Leitch CC, Kim JC, Ross AJ, Eichers ER, Teslovich TM, Mah AK, Johnsen RC, Cavender JC, Lewis RA, Leroux MR, Beales PL, Katsanis N (2003) Basal body dysfunction is a likely cause of pleiotropic Bardet-Biedl syndrome. Nature 425:628–633

Badano JL, Kim JC, Hoskins BE, Lewis RA, Ansley SJ, Cutler DJ, Castellan C, Beales PL, Leroux MR, Katsanis N (2003) Heterozygous mutations in *BBS1*, *BBS2* and *BBS6* have a potential epistatic effect on Bardet-Biedl patients with two mutations at a second BBS locus. Hum Mol Genet 12:1651–1659

Badano JL, Leitch CC, Ansley SJ, May-Simera H, Lawson S, Lewis RA, Beales PL, Dietz HC, Fisher S, Katsanis N (2006) Dissection of epistasis in oligogenic Bardet-Biedl syndrome. Nature 439:326–330

Bähler M, Rhoads A (2002) Calmodulin signaling via the IQ motif. FEBS Lett 513:107–113

Beales PL, Elcioglu N, Woolf AS, Parker D, Flinter FA (1999) New criteria for improved diagnosis of Bardet-Biedl syndrome: results of a population survey. J Med Genet 36:437–446

Beales PL, Badano JL, Ross AJ, Ansley SJ, Hoskins BE, Kirsten B, Mein CA, Froguel P, Scambler PJ, Lewis RA, Lupski JR, Katsanis N (2003) Genetic interaction of BBS1 mutations with alleles at other BBS loci can result in non-Mendelian Bardet-Biedl syndrome. Am J Hum Genet 72:1187–1199

Biegert A, Söding J (2009) Sequence context-specific profiles for homology searching. Proc Natl Acad Sci USA 106:3770–3775

Bin J, Madhavan J, Ferrini W, Mok CA, Billingsley G, Héon E (2009) BBS7 and TTC8 (BBS8) mutations play a minor role in the mutational load of Bardet-Biedl syndrome in a multiethnic population. Hum Mutat 30:E737–E746

Burkhard P, Stetefeld J, Strelkov SV (2001) Coiled coils: a highly versatile protein folding motif. Trends Cell Biol 11:82–88

Cardenas-Rodriguez M, Badano JL (2009) Ciliary biology: understanding the cellular and genetic basis of human ciliopathies. Am J Med Genet Part C Semin Med Genet 151C:263–280

Davis EE, Brueckner M, Katsanis N (2006) The emerging complexity of the vertebrate cilium: new functional roles for an ancient organelle. Dev Cell 11:9–19

Dinkel H, Michael S, Weatheritt RJ, Davey NE, Van Roey K, Altenberg B, Toedt G, Uyar B, Seiler M, Budd A, Jödicke L, Dammert MA, Schroeter C, Hammer M, Schmidt T, Jehl P, McGuigan C, Dymecka M, Chica C, Luck K, Via A, Chatr-Aryamontri A, Haslam N, Grebnev G, Edwards RJ, Steinmetz MO, Meiselbach H, Diella F, Gibson TJ (2012) ELM—the database of eukaryotic linear motifs. Nucleic Acid Res 40:D242–D251

Essner JJ, Amack JD, Nyholm MK, Harris EB, Yost HJ (2005) Kupffer's vesicle is a ciliated organ of asymmetry in the zebrafish embryo that initiates left-right development of the brain, heart and gut. Development 132:1247–1260

Fan Y, Esmail MA, Ansley SJ, Blacque OE, Boroevich K, Ross AJ, Moore SJ, Badano JL, May-Simera H, Compton DS, Green JS, Lewis RA, van Haelst MM, Parfrey PS, Baillie DL, Beales PL, Katsanis N, Davidson WS, Leroux MR (2004) Mutations in a member of the Ras superfamily of small GTP-binding proteins causes Bardet-Biedl syndrome. Nat Genet 36:989–993

Fath MA, Mullins RF, Searby C, Nishimura DY, Wei J, Rahmouni K, Davis RE, Tayeh MK, Andrews M, Yang B, Sigmund CD, Stone EM, Sheffield VC (2005) Mkks-null mice have a phenotype resembling Bardet-Biedl syndrome. Hum Mol Genet 14:1109–1118

Flicek P, Amode MR, Barrell D, Beal K, Brent S, Chen Y, Clapham P, Coates G, Fairley S, Fitzgerald S, Gordon L, Hendrix M, Hourlier T, Johnson N, Kähäri A, Keefe D, Keenan S, Kinsella R, Kokocinski F, Kulesha E, Larsson P, Longden I, McLaren W, Overduin B, Pritchard B, Riat HS, Rios D, Ritchie GR, Ruffier M, Schuster M, Sobral D, Spudich G, Tang YA, Trevanion S, Vandrovcova J, Vilella AJ, White S, Wilder SP, Zadissa A, Zamora J, Aken BL, Birney E, Cunningham F, Dunham I, Durbin R, Fernández-Suarez XM, Herrero J, Hubbard TJ, Parker A, Proctor G, Vogel J, Searle SM (2011) Ensembl 2011. Nucleic Acid Res 39:D800–D806

Gascue C, Tan PL, Cardenas-Rodriguez M, Libisch G, Fernandez-Calero T, Liu YP, Astrada S, Robello C, Naya H, Katsanis N, Badano JL (2012) Direct role of Bardet-Biedl syndrome proteins in transcriptional regulation. J Cell Sci 125:362–375

Gerdes JM, Liu Y, Zaghloul NA, Leitch CC, Lawson SS, Kato M, Beachy PA, Beales PL, Demartino GN, Fisher S, Badano JL, Katsanis N (2007) Disruption of the basal body compromises proteasomal function and perturbs intracellular Wnt response. Nat Genet 39:1350–1360

Guindon S, Gascuel O (2003) A simple, fast, and accurate algorithm to estimate large phylogenies by maximum likelihood. Syst Biol 52:696–704

Ibanez-Tallon I, Pagenstecher A, Fliegauf M, Olbrich H, Kispert A, Ketelsen UP, North A, Heintz N, Omran H (2004) Dysfunction of axonemal dynein heavy chain Mdnah5 inhibits ependymal flow and reveals a novel mechanism for hydrocephalus formation. Hum Mol Genet 13:2133–2141

Jin H, White SR, Shida T, Schulz S, Aguiar M, Gygi SP, Bazan JF, Nachury MV (2010) The conserved Bardet-Biedl syndrome proteins assemble a coat that traffics membrane proteins to cilia. Cell 141:1208–1219

Katoh K, Misawa K, Kuma K, Miyata T (2002) MAFFT: a novel method for rapid multiple sequence alignment based on fast Fourier transform. Nucleic Acid Res 30:3059–3066

Katsanis N, Ansley SJ, Badano JL, Eichers ER, Lewis RA, Hoskins BE, Scambler PJ, Davidson WS, Beales PL, Lupski JR (2001) Triallelic inheritance in Bardet-Biedl syndrome, a Mendelian recessive disorder. Science 293:2256–2259

Kim JC, Badano JL, Sibold S, Esmail MA, Hill J, Hoskins BE, Leitch CC, Venner K, Ansley SJ, Ross AJ, Leroux MR, Katsanis N, Beales PL (2004) The Bardet-Biedl protein BBS4 targets cargo to the pericentriolar region and is required for microtubule anchoring and cell cycle progression. Nat Genet 36:462–470

Kim JC, Ou YY, Badano JL, Esmail MA, Leitch CC, Fiedrich E, Beales PL, Archibald JM, Katsanis N, Rattner JB, Leroux MR (2005) MKKS/BBS6, a divergent chaperonin-like protein linked to the obesity disorder Bardet-Biedl syndrome, is a novel centrosomal component required for cytokinesis. J Cell Sci 118:1007–1020

Kim SK, Shindo A, Park TJ, Oh EC, Ghosh S, Gray RS, Lewis RA, Johnson CA, Attie-Bittach T, Katsanis N, Wallingford JB (2010) Planar cell polarity acts through septins to control collective cell movement and ciliogenesis. Science 329:1337–1340

Kramer-Zucker AG, Olale F, Haycraft CJ, Yoder BK, Schier AF, Drummond IA (2005) Cilia-driven fluid flow in the zebrafish pronephros, brain and Kupffer's vesicle is required for normal organogenesis. Development 132:1907–1921

Laurier V, Stoetzel C, Muller J, Thibault C, Corbani S, Jalkh N, Salem N, Chouery E, Poch O, Licaire S, Danse JM, Amati-Bonneau P, Bonneau D, Mégarbané A, Mandel JL, Dollfus H (2006) Pitfalls of homozygosity mapping: an extended consanguineous Bardet-Biedl syndrome family with two mutant genes (BBS2, BBS10), three mutations, but no triallelism. Eur J Hum Genet 14:1195–1203

Leitch CC, Zaghloul NA, Davis EE, Stoetzel C, Diaz-Font A, Rix S, Al-Fadhel M, Lewis RA, Eyaid W, Banin E, Dollfus H, Beales PL, Badano JL, Katsanis N (2008) Hypomorphic mutations in syndromic encephalocele genes are associated with Bardet-Biedl syndrome. Nat Genet 40:443–448

Li JB, Gerdes JM, Haycraft CJ, Fan Y, Teslovich TM, May-Simera H, Li H, Blacque OE, Li L, Leitch CC, Lewis RA, Green JS, Parfrey PS, Leroux MR, Davidson WS, Beales PL, Guay-Woodford LM, Yoder BK, Stormo GD, Katsanis N, Dutcher SK (2004) Comparative genomic identification of conserved flagellar and basal body proteins that includes a novel gene for Bardet-Biedl syndrome. Cell 117:541–552

Loktev AV, Zhang Q, Beck JS, Searby CC, Scheetz TE, Bazan JF, Slusarski DC, Sheffield VC, Jackson PK, Nachury MV (2008) A BBSome subunit links ciliogenesis, microtubule stability, and acetylation. Dev Cell 15:854–865

Loytynoja A, Goldman N (2005) An algorithm for progressive multiple alignment of sequences with insertions. Proc Natl Acad Sci U S A 102:10557–10562

Lupas A, Van Dyke M, Stock J (1991) Predicting coiled coils from protein sequences. Science 252:1162–1164

Marion V, Stoetzel C, Schlicht D, Messaddeq N, Koch M, Flori E, Danse JM, Mandel JL, Dollfus H (2009) Transient ciliogenesis involving Bardet-Biedl syndrome proteins is a fundamental

characteristic of adipogenic differentiation. Proc Natl Acad Sci USA 10:1820–1825

Marion V, Stutzmann F, Gérard M, De Melo C, Schaefer E, Claussmann A, Hellé S, Delague V, Souied E, Barrey C, Verloes A, Stoetzel C, Dollfus H (2012) Exome sequencing identifies mutations in LZTFL1, a BBSome and smoothened trafficking regulator, in a family with Bardet–Biedl syndrome with situs inversus and insertional polydactyly. J Med Genet 49:317–321

May-Simera HL, Ross A, Rix S, Forge A, Beales PL, Jagger DJ (2009) Patterns of expression of Bardet-Biedl syndrome proteins in the mammalian cochlea suggest noncentrosomal functions. J Comp Neurol 514:174–188

May-Simera HLKM, Hernandez V, Osborn DP, Tada M, Beales PL (2010) Bbs8, together with the planar cell polarity protein Vangl2, is required to establish left-right asymmetry in zebrafish. Dev Biol 345:215–225

Mykytyn K, Mullins RF, Andrews M, Chiang AP, Swiderski REç, Yang B, Braun T, Casavant T, Stone EM, Sheffield VC (2004) Bardet-Biedl syndrome type 4 (BBS4)-null mice implicate Bbs4 in flagella formation but not global cilia assembly. Proc Natl Acad Sci USA 101:8664–8669

Nachury MV, Loktev AV, Zhang Q, Westlake CJ, Peränen J, Merdes A, Slusarski DC, Scheller RH, Bazan JF, Sheffield VC, Jackson PK (2007) A core complex of BBS proteins cooperates with the GTPase Rab8 to promote ciliary membrane biogenesis. Cell 129:1201–1213

Nido GS, Méndez R, Pascual-García A, Abia D, Bastolla U (2012) Protein disorder in the centrosome correlates with complexity in cell types number. Mol BioSyst 8:353–367

Nishimura DY, Fath M, Mullins RF, Searby C, Andrews M, Davis R, Andorf JL, Mykytyn K, Swiderski RE, Yang B, Carmi R, Stone EM, Sheffield VC (2004) Bbs2-null mice have neurosensory deficits, a defect in social dominance, and retinopathy associated with mislocalization of rhodopsin. Proc Natl Acad Sci USA 101:16588–16593

Notredame C, Higgins DG, Heringa J (2000) T-Coffee: a novel method for fast and accurate multiple sequence alignment. J Mol Biol 302:205–217

Otto EA, Hurd TW, Airik R, Chaki M, Zhou W, Stoetzel C, Patil SB, Levy S, Ghosh AK, Murga-Zamalloa CA, van Reeuwijk J, Letteboer SJF, Sang L, Giles RH, Liu Q, Coene KLM, Estrada-Cuzcano A, Collin RWJ, McLaughlin HM, Held S, Kasanuki JM, Ramaswami G, Conte J, Lopez I, Washburn J, MacDonald J, Hu J, Yamashita Y, Maher ER, Guay-Woodford L, Neumann HPH, Obermüller N, Koenekoop RK, Bergmann C, Bei X, Lewis RA, Katsanis N, Lopes V, Williams DS, Lyons RH, Dang CV, Brito DA, Bettencourt Dias M, Zhang X, Cavalcoli JD, Nürnberg G, Nürnberg P, Pierce EA, Jackson P, Antignac C, Saunier S, Roepman R, Dollfus H, Khanna H, Hildebrandt F (2010) Candidate exome capture identifies mutation of SDCCAG8 as the cause of a retinal-renal ciliopathy. Nat Genet 42:840–850

Petit A, Ragu C, Soler G, Ottolenghi C, Schluth C, Radford-Weiss I, Schneider-Maunoury S, Callebaut I, Dastugue N, Drabkin HA, Bernard OA, Romana S, Penard-Lacronique V (2012) Functional analysis of the NUP98-CCDC28A fusion protein. Haematologica 97:379–387

Redin C, Le Gras S, Mhamdi O, Geoffroy V, Stoetzel C, Vincent MC, Chiurazzi P, Lacombe D, Ouertani I, Petit F, Till M, Verloes A, Jost B, Chaabouni HB, Dollfus H, Mandel JL, Muller J (2012) Targeted high-throughput sequencing for diagnosis of genetically heterogeneous diseases: efficient mutation detection in Bardet-Biedl and Alstrom Syndromes. J Med Genet 49:502–512

Remmert M, Biegert A, Hauser A, Söding J (2011) HHblits: lightning-fast iterative protein sequence searching by HMM–HMM alignment. Nat Methods 9:173–175

Ross AJ, May-Simera H, Eichers ER, Kai M, Hill J, Jagger DJ, Leitch CC, Chapple JP, Munro PM, Fisher S, Tan PL, Phillips HM, Leroux MR, Henderson DJ, Murdoch JN, Copp AJ, Eliot MM, Lupski JR, Kemp DT, Dollfus H, Tada M, Katsanis N, Forge A, Beales PL (2005) Disruption of Bardet-Biedl syndrome ciliary proteins perturbs planar cell polarity in vertebrates. Nat Genet 37:1135–1140

Seo S, Baye LM, Schulz NP, Beck JS, Zhang Q, Slusarski DC, Sheffield VC (2010) BBS6, BBS10, and BBS12 form a complex with CCT/TRiC family chaperonins and mediate BBSome assembly. Proc Natl Acad Sci USA 107:1488–1493

Smaoui N, Chaabouni M, Sergeev YV, Kallel H, Li S, Mahfoudh N, Maazoul F, Kammoun H, Gandoura N, Bouaziz A, Nouiri E, M'Rad R, Chaabouni H, Hejtmancik JF (2006) Screening of the eight BBS genes in Tunisian families: no evidence of triallelism. Invest Ophthalmol Vis Sci 47:3487–3495

Söding J (2005) Protein homology detection by HMM–HMM comparison. Bioinformatics 21:951–960

Söding J, Remmert M, Biegert A, Lupas AN (2006) HHsenser: exhaustive transitive profile search using HMM–HMM comparison. Nucleic Acid Res 34:W374–W378

Stoetzel C, Laurier V, Davis EE, Muller J, Rix S, Badano JL, Leitch CC, Salem N, Chouery E, Corbani S, Jalk N, Vicaire S, Sarda P, Hamel C, Lacombe D, Holder M, Odent S, Holder S, Brooks AS, Elcioglu NH, Silva ED, Rossillion B, Sigaudy S, de Ravel TJ, Lewis RA, Leheup B, Verloes A, Amati-Bonneau P, Mégarbané A, Poch O, Bonneau D, Beales PL, Mandel JL, Katsanis N, Dollfus H (2006) BBS10 encodes a vertebrate-specific chaperonin-like protein and is a major BBS locus. Nat Genet 38:521–524

Stoetzel C, Muller J, Laurier V, Davis EE, Zaghloul NA, Vicaire S, Jacquelin C, Plewniak F, Leitch CC, Sarda P, Hamel C, de Ravel TJ, Lewis RA, Friederich E, Thibault C, Danse JM, Verloes A, Bonneau D, Katsanis N, Poch O, Mandel JL, Dollfus H (2007) Identification of a novel BBS gene (BBS12) highlights the major role of a vertebrate-specific branch of chaperonin-related proteins in Bardet-Biedl syndrome. Am J Hum Genet 80:1–11

The Uniprot Consortium TU (2012) Reorganizing the protein space at the Universal Protein Resource (UniProt). Nucleic Acid Res 40:D71–D75

Tobin JL, Di Franco M, Eichers E, May-Simera H, Garcia M, Yan J, Quinlan R, Justice MJ, Hennekam RC, Briscoe J, Tada M, Mayor R, Burns AJ, Lupski JR, Hammond P, Beales PL (2008) Inhibition of neural crest migration underlies craniofacial dysmorphology and Hirschsprung's disease in Bardet-Biedl syndrome. Proc Natl Acad Sci USA 105:6714–6719

Veland IR, Awan A, Pedersen LB, Yoder BK, Christensen ST (2009) Primary cilia and signaling pathways in mammalian development, health and disease. Nephron Physiol 111:39–53

Veleri S, Bishop K, Dalle Nogare DE, English MA, Foskett TJ, Chitnis A, Sood R, Liu P, Swaroop A (2012) Knockdown of Bardet-Biedl syndrome gene BBS9/PTHB1 leads to cilia defects. PLoS ONE 7:e34389

Walczak-Sztulpa J, Eggenschwiler J, Osborn D, Brown DA, Emma F, Klingenberg C, Hennekam RC, Torre G, Garshasbi M, Tzschach A, Szczepanska M, Krawczynski M, Zachwieja J, Zwolinska D, Beales PL, Ropers HH, Latos-Bielenska A, Kuss AW (2010) Cranioectodermal Dysplasia, Sensenbrenner syndrome, is a ciliopathy caused by mutations in the IFT122 gene. Am J Hum Genet 86:949–956

Ward JJ, Sodhi JS, McGuffin LJ, Buxton BF, Jones DT (2004) Prediction and functional analysis of native disorder in proteins from the three kingdoms of life. J Mol Biol 337:635–645

Waterhouse AM, Procter JB, Martin DM, Clamp M, Barton GJ (2009) Jalview Version 2—a multiple sequence alignment editor and analysis workbench. Bioinformatics 25:1189–1191

Wiens CJ, Tong Y, Esmail MA, Oh E, Gerdes JM, Wang J, Tempel W, Rattner JB, Katsanis N, Park HW, Leroux MR (2010) Bardet-Biedl syndrome-associated small GTPase ARL6 (BBS3) functions at or near the ciliary gate and modulates Wnt signaling. J Biol Chem 285:16218–16230

Yen HJ, Tayeh MK, Mullins RF, Stone EM, Sheffield VC, Slusarski DC (2006) Bardet-Biedl syndrome genes are important in retrograde intracellular trafficking and Kupffer's vesicle cilia function. Hum Mol Genet 15:667–677

Zhang Q, Seo S, Bugge K, Stone EM, Sheffield VC (2012) BBS proteins interact genetically with the IFT pathway to influence SHH-related phenotypes. Hum Mol Genet 21:1945–1953